Magnetic properties and surface domain structure of $(Nd_{0.85}Dy_{0.15})_{10}Fe_{83}Zr_1B_6$ thin ribbons

Agnieszka CEGLAREK[1*], Danuta PŁUSA[1], Marcin DOŚPIAŁ[1],
Marcin NABIAŁEK[1], Paweł WIECZOREK[2]

[1]Institute of Physics, Częstochowa University of Technology,
 al. Armii Krajowej 19, 42 200 Częstochowa, Poland

[2]Institute of Materials Engineering, Częstochowa University of Technology,
 al. Armii Krajowej 19, 42 200 Częstochowa, Poland

*Corresponding author: a.ceglarek@go2.pl

In this paper, the nanocrystalline $(Nd_{0.85}Dy_{0.15})_{10}Fe_{83}Zr_1B_6$ ribbons produced by melt-spinning have been investigated by the X-ray diffraction method (XRD), vibrating sample magnetometer (VSM) and magnetic force microscopy (MFM). The XRD studies showed that material investigated was mainly composed of $Re_2Fe_{14}B$ and α-Fe phases with fine grain sizes of 25 and 9 nm, respectively. The magnetic parameters determined from the hysteresis loop measurements are as follows: $\mu_0 H_C = 0.96$ T, $\mu_0 M_R = 0.76$ T, $\mu_0 M_S = 1.09$ T, $(BH)_{max} = 88$ kJ/m^3. The large remanence ratio ($\mu_0 M_R/\mu_0 M_S$) of 0.7 results from the exchange coupling between the soft and hard magnetic grains. The large surface interaction domains revealed by MFM confirmed the existence of strong exchange coupling between nanosize grains.

Keywords: nanocomposite materials, melt-spinning method, Re–Fe–B alloys, hard magnetic magnets, surface domain structure.

1. Introduction

Modern nanocomposites obtained on the basis of $Re_2Fe_{14}B$ (Re = Nd, Dy, Pr) and α-Fe phases are characterized by excellent functional parameters and belong to the latest generation of the hard magnetic materials. The article describes research on nanocrystalline Nd–Fe–B-type ribbons produced by the melt-spinning method. The melt-spinning method is a simple and economical way to prepare nanocomposite ribbons, which can be used for obtaining the hard magnetic materials. These nanocomposite magnets are produced from alloys which have a lowered amount of neodymium compared to the composition of magnetically hard $Nd_2Fe_{14}B$ phase. These materials, due to a unique microstructure which consists of exchange interacting hard and soft magnetic phases, are characterized by high density of maximum energy product $(BH)_{max}$ and enhanced

remanence $\mu_0 M_R$. In order to compensate the decreasing in coercivity caused by the exchange interaction, the neodymium atoms are replaced by a small amount of dysprosium (Dy = 0.5–2 at.%), since the anisotropy field of $Dy_2Fe_{14}B$ phase is higher than the anisotropy field of $Nd_2Fe_{14}B$ phase [1, 2]. It must be noted that the addition of zirconium influences the exchange interactions and significantly affects the magnetic properties [3, 4].

In nanocomposite magnets with a very fine grain size (less than 40 nm) the large interaction domains are formed due to the strong magnetic interaction between grains. The number of works dealing with the investigation of the interaction domains and correlation between them and microstructure and magnetic properties is limited [5–8].

In this paper the magnetic properties and surface interaction domains structure of $(Nd_{0.85}Dy_{0.15})_{10}Fe_{83}Zr_1B_6$ thin ribbons are presented.

2. Research methodology; studied materials

The samples of $(Nd_{0.85}Dy_{0.15})_{10}Fe_{83}Zr_1B_6$ were obtained from high purity elements using the arc melting in the protective argon atmosphere. A small amount of Zr (1 at.%) was added in order to hinder the grain growth. The nanocomposite ribbons were prepared by rapid quenching of the liquid alloy on a rotating cooper wheel with the linear velocity of 20 m/s and pressure inside the chamber of 0.4×10^5 Pa.

The phase composition was determined using a Bruker D8 Advance X-ray diffractometer with Lynx Eye semiconductor counter and CuK_α as a radiation source. The Scherrer formula was used to calculate the average grain size from the peaks broadening.

The hysteresis loop was measured under magnetic field up to 2 T using the LakeShore vibrating sample magnetometer at room temperature. The magnetic field was applied along the longitudinal direction of the ribbon. From the major hysteresis loop, the magnetic parameters, *i.e.*: coercivity $\mu_0 H_C$, remanence $\mu_0 M_R$, saturation magnetization $\mu_0 M_S$, and maximum energy product $(BH)_{max}$, were determined.

The study of the domain structure was carried out using magnetic force microscopy (MFM). The magnetic contrast imaging was performed in tapping (AFM – topography of sample surface)/lift (MFM – magnetic structure) mode. The MESP-ESP tip coated with CoCr films of thickness of ~50 nm with coercivity of 32 kA/m and at a scan height of 40 nm was employed. The tip was magnetized along the tip axis perpendicular to the ribbon surface.

3. Results and discussion

Figure 1 shows the X-ray diffractogram for the sample in an as-cast state. The diffractogram shows peaks corresponding to α-Fe and $Re_2Fe_{14}B$ phases with a wide and visible amorphous halo. Using the Scherrer formula, the average grain sizes of both α-Fe and $Re_2Fe_{14}B$ phases were estimated as equal to 9 and 25 nm, respectively.

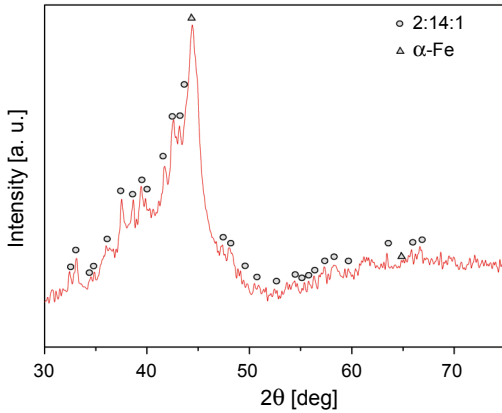Fig. 1. X-ray diffractogram $(Nd_{0.85}Dy_{0.15})_{10}Fe_{83}Zr_1B_6$ ribbon in the as-cast state.
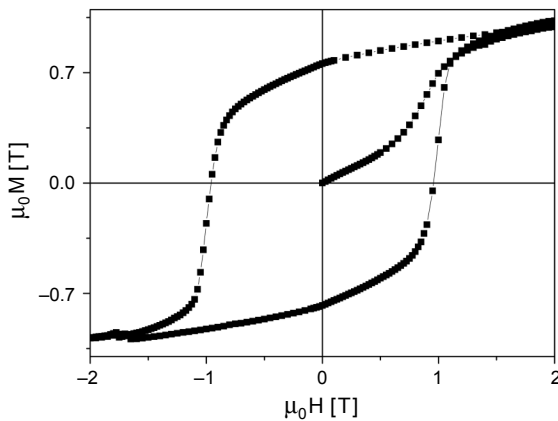

Fig. 2. Hysteresis loop of $(Nd_{0.85}Dy_{0.15})_{10}Fe_{83}Zr_1B_6$ ribbon in the as-cast state.

In Figure 2 the hysteresis loop measured at a magnetic field of 2 T is presented. From this loop, the values of coercivity, remanence and maximum energy product were evaluated to be: $\mu_0 H_C = 0.96$ T, $\mu_0 M_R = 0.76$ T, $(BH)_{max} = 88$ kJ/m^3. The saturation magnetization $\mu_0 M_S = 1.09$ T was obtained from the plot of $\mu_0 M$ versus $1/(\mu_0 H)^2$ by extrapolating the curve to $1/(\mu_0 H)^2 = 0$.

As it can be seen from Fig. 2, the initial magnetization curve rises gradually at low fields, exhibiting an inflection point at a field about 0.7 T and then rises more rapidly. The observed shape of the initial magnetization curve results from the combination of different reversal magnetization mechanisms like the rotation of the magnetic moments for lower and pinning of domain walls for higher values of applied magnetic fields. The hysteresis loop of the ribbons investigated shows a single-phase behaviour and a good rectangularity. The demagnetization curve shape is typical for multi-phase material with strong exchange interaction between grains of magnetically soft and
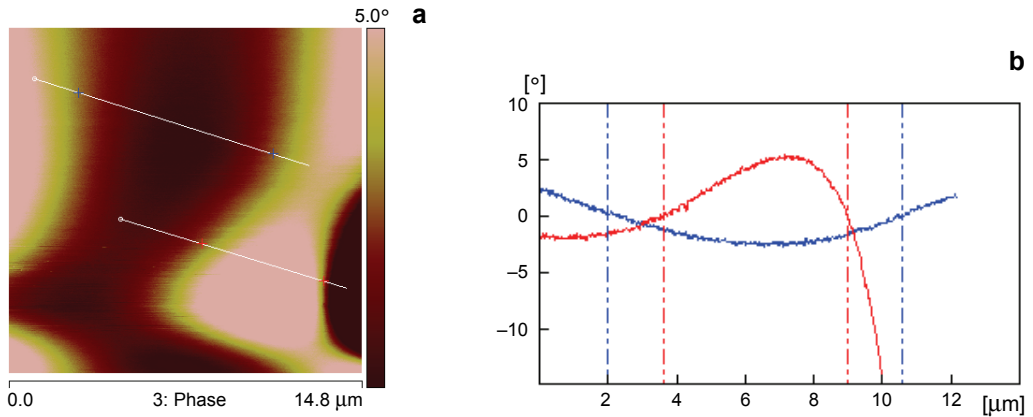
Fig. 3. MFM image of nanocomposite $(Nd_{0.85}Dy_{0.15})_{10}Fe_{83}Zr_1B_6$ ribbon in the as-cast state (**a**), line section from MFM image (**b**).

hard phases. This is also confirmed by the high remanence ratio of 0.7, which is larger than 0.5 (according to the Stoner–Wohlfarth theory for single domain non-interacting particles [9]).

Figure 3**a** presents the magnetic domain structure image observed by MFM with a scan size 14.8 µm×14.8 µm. From two scan lines (Fig. 3**b**) corresponding to MFM image, the magnetic domain width taken at different places was measured as equal to 8.61 µm for dark domain (negative phase shift corresponding to an attractive interaction between the tip and the sample surface) and 5.36 µm for light domain (positive phase shift corresponding to a repellent interaction between the tip and the sample surface). Light and dark domains mean that they are magnetized oppositely perpendicular to the sample surface. The nature of theses domains is different than that of classical domains with 180° Bloch walls. The magnetic domains extend over
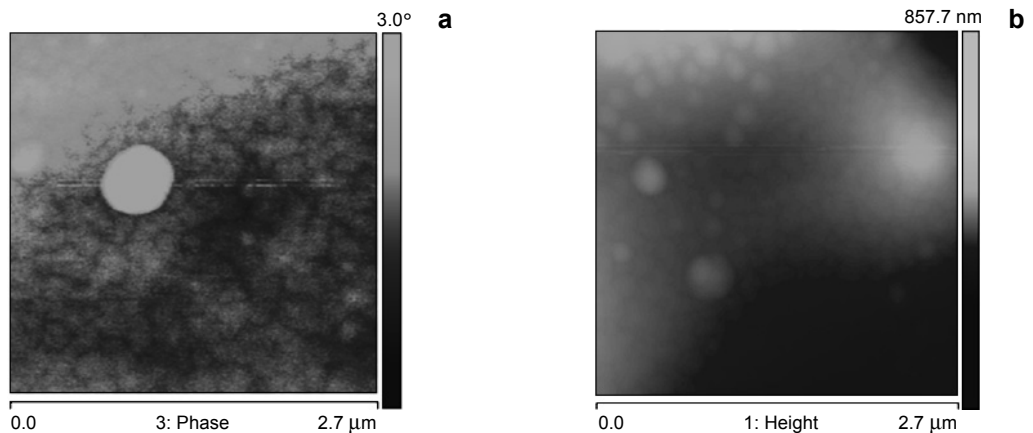

Fig. 4. MFM image of nanocomposite $(Nd_{0.85}Dy_{0.15})_{10}Fe_{83}Zr_1B_6$ ribbon (**a**), AFM image corresponding to MFM image from Fig. 4**a** (**b**).

the area consisting of hundreds of grains whose sizes (25 nm) are much smaller than the single-domain diameter for $Re_2Fe_{14}B$ phase (190 nm [10]), which means that they are the interaction domains.

The interaction domains observed in this work are ten or more times larger than those reported for example in [5, 6] for nanocomposites with another composition. This proves that the exchange interactions in the sample investigated are very strong.

In a MFM image presented in Fig. 4**a** the fine structure with sizes comparable to grains diameter can be seen within the interaction domains certifying that the interaction domains are composed of many single-domain grains with slightly different magnetization direction. The contrast within the interaction domains is not homogenous. Figure 4**b** presents the AFM image corresponding to MFM one in which the same details are visible but the contrast is much weaker, which means that the details visible in MFM image are not of magnetic origin.

4. Conclusions

Based on the research, the following conclusions can be drawn:

– The ribbons examined are multi-phase, consisting of the magnetically hard $Re_2Fe_{14}B$, soft α-Fe and amorphous phases;

– Demagnetization curves are smooth and single-stage like in single-phase material;

– The ratio $\mu_0 M_R / \mu_0 M_S = 0.7$ proves that nanosize grains are strong exchange coupled;

– The interaction domains revealed by MFM method confirm the existence of strong exchange interaction between grains.

References

[1] THE N.D., HOA N.Q., OH S.K., YU S.C., ANH H.D., VU L.V., CHAU N., *Crystalline evolution and large coercivity in Dy-doped (Nd,Dy)$_2$Fe$_{14}$B/α-Fe nanocomposite magnets*, Journal of Physics D: Applied Physics **40**(1), 2007, pp. 119–122.

[2] ZHONGMIN CHEN, OKUMURA H., HADJIPANAYIS G.C., QUN CHEN, *Enhacement of magnetic properties of nanocomposite Pr$_2$Fe$_{14}$B/α-Fe magnets by small substitution of Dy for Pr*, Journal of Applied Physics **89**(4), 2001, pp. 2299–2303.

[3] WANG C., YAN M., LI Q., *Effects of Nd and B contents on the thermal stability of nanocomposite (Nd,Zr)$_2$Fe$_{14}$B/α-Fe magnets*, Materials Science and Engineering B **150**(1), 2008, pp. 77–82.

[4] XIAOQIAN BAO, JIE ZHU, WEI LI, XUEXU GAO, SHOUZENG ZHOU, *Influence of zirconium addition on microstructure, magnetic properties and thermal stability of nanocrystalline Nd$_{12.3}$Fe$_{81.7}$B$_{6.0}$ alloy*, Journal of Rare Earths **27**(5), 2009, pp. 843–847.

[5] DOŚPIAŁ M., PŁUSA D., ŚLUSAREK B., *Study of the magnetic interaction in nanocrystalline Pr–Fe–Co––Nb–B permanent magnets*, Journal of Magnetism and Magnetic Materials **324**(5), 2012, pp. 843–848.

[6] SZMAJA W., GROBELNY J., CICHOMSKI M., HIROSAWA S., SHIGEMOTO Y., *Magnetic force microscopy investigation of the domain structure of nanocomposite Nd$_2$Fe$_{14}$B/ Fe$_3$B magnets*, Acta Materialia **59**(2), 2011, pp. 531–536.

[7] AL-KHAFAJI M.A., RAINFORTH W.M., GIBBS M.R.J., DAVIES H.A., BISHOP J.E.L., *Magnetic force microscopy of nanocrystalline NdFeB ribbons: A study of tip-sample interaction using a well--characterized sample*, Journal of Magnetism and Magnetic Materials **182**(1–2), 1998, pp. 111–123.

[8] AL-KHAFAJI M.A., RAINFORTH W.M., GIBBS M.R.J., DAVIES H.A., BISHOP J.E.L., *The effect of phase constitution on the magnetic structure of nanophase NdFeB alloys observed by magnetic force microscopy*, Journal of Magnetism and Magnetic Materials **188**(1–2), 1998, pp. 109–118.

[9] STONER E.C., WOHLFARTH W.P., *A mechanism of magnetic hysteresis in heterogeneous alloys*, Philosophical Transactions of the Royal Society A **240**(826), 1948, pp. 599–642.

[10] GRÖNEFELD M., KRONMÜLLER H., *Initial magnetization curve and hardening mechanism in rapidly quenched NdFeB magnets*, Journal of Magnetism and Magnetic Materials **88**(3), 1990, pp. L267–L274.